Inorganic Chemistry
Article
Cite This: Inorg. Chem. XXXX, XXX, XXX−XXX
pubs.acs.org/IC

Coordination of 2,2′-(Trifluoroazanediyl)bis(*N*,*N*′-dimethylacetamide) with U(VI), Nd(III), and Np(V): A Thermodynamic and Structural Study

Yang Gao,[†,‡] Bernard F. Parker,[†,§] Phuong V. Dau,[†] Phuong D. Dau,[†] Trevor D. Lohrey,[†,§] John K. Gibson,[†] John Arnold,[†,§] Simon J. Teat,[⊥] Andrea Melchior,[¶] Zhicheng Zhang,[*,†] and Linfeng Rao[*,†]

[†] Chemical Sciences Division, Lawrence Berkeley National Laboratory, 1 Cyclotron Road, Berkeley, California 94720, United States
[‡] College of Nuclear Science and Technology, Harbin Engineering University, Harbin 150001, China
[§] Department of Chemistry, University of California − Berkeley, Berkeley, California 94720, United States
[⊥] Advanced Light Source, Lawrence Berkeley National Laboratory, 1 Cyclotron Road, Berkeley, California 94720, United States
[¶] Dipartimento Politecnico di Ingegneria e Architettura, Università di Udine, Laboratori di Chimica, via delle Scienze 99, 33100 Udine, Italy

Supporting Information

ABSTRACT: Thermodynamic properties of the complexation of 2,2′-(trifluoroazanediyl)bis(*N*,*N*′-dimethylacetamide) (CF_3ABDMA) with U(VI), Nd(III), and Np(V) have been studied in 1.0 M $NaNO_3$ at 25 °C. Equilibrium constants of the complexation were determined by potentiometry and spectrophotometry. In comparison with a series of structurally related amine-bridged diacetamide ligands, including 2,2′-(benzylazanediyl)bis(*N*,*N*′-dimethylacetamide) (BnABDMA), 2,2′-azanediylbis(N,*N*′-dimethylacetamide) (ABDMA), and 2,2′-(methylazanediyl)bis(*N*,*N*′-dimethylacetamide) (MABDMA), CF_3ABDMA forms weaker complexes with U(VI), Nd(III), and Np(V) due to the lower basicity of the center N atom in CF_3ABDMA resulting from the attachment of the strong electron-withdrawing CF_3- moiety. The complexation strength of CF_3ABDMA with the three metal ions follows the order: $UO_2^{2+} > Nd^{3+} > NpO_2^{+}$, consistent with the order of the "effective" charges of the metal ions. Structural information on the U(VI)/CF_3ABDMA complexes in solution and in solid was obtained by theoretical computation, single crystal X-ray diffractometry, ^{19}F NMR, and electrospray ionization mass spectrometry. The structural data indicate that, similar to the three previously studied amine-bridged diacetamide ligands (BnABDMA, ABDMA, and MABDMA), the CF_3ABDMA ligand coordinates to UO_2^{2+} in a tridentate mode, through the center nitrogen and the two amide oxygen atoms.

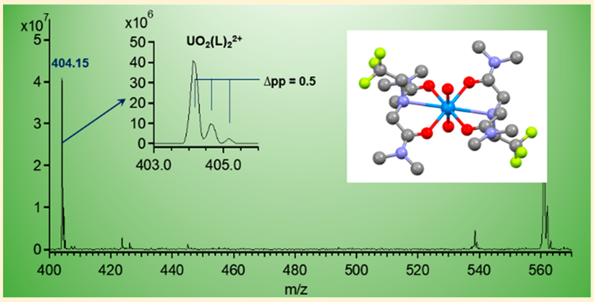

1. INTRODUCTION

Large quantities of minor actinides (MAs = Am, Np, and *Cm*) and fission products including trivalent lanthanides (Ln(III)) coexist in high level nuclear waste (HLW) generated during the reprocessing of spent nuclear fuel. Efficient separation of these radioactive elements from HLW can not only recover valuable isotopes but also reduce the long-term heat loading and radioactive hazards in HLW, which is very beneficial to the final treatment and disposal of the nuclear wastes in geological repositories.

In an advanced nuclear fuel cycle, a strategy of partitioning and transmutation (P&T)[1,2] is proposed. With the P&T strategy, the long-lived minor actinides are separated from the trivalent lanthanides and converted into isotopes that are stable or short-lived. For the success of P&T strategy in the advanced nuclear fuel cycle, the separation of ^{237}Np should be emphasized because of its long half-life and high radiation hazard. For example, in the HLW, ^{237}Np is predicted to become a major radiation contributor among the long-lived radionuclides, contributing 67% of the total radiation dose from HLW 75 000 years after the closure of the repository.[3] The pentavalent state of neptunium, Np(V), is the most stable oxidation state and exists as NpO_2^+ ions in solution.[4] Because of its low ionic charge and large ionic radius, NpO_2^+ has a weak tendency toward hydrolysis, precipitation, or sorption by geomedia so that it is highly mobile in the environment.[4] Also, NpO_2^+ does not form strong complexes with many ligands and is difficult to separate by many traditional extracting agents in actinide separation processes. Besides neptunium, separation of trivalent actinides (An(III)) from lanthanides is a challenging task because of the extremely high similarity of their chemical

Received: August 14, 2019

DOI: 10.1021/acs.inorgchem.9b02469
Inorg. Chem. XXXX, XXX, XXX−XXX

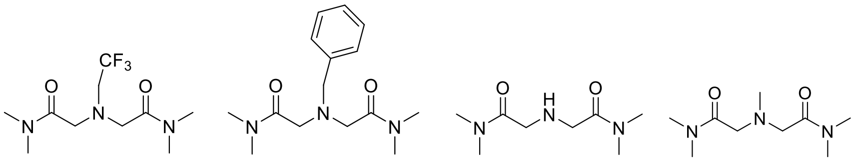

Figure 1. From left to right: CF_3ABDMA (this work), BnABDMA, ABDMA, and MABDMA.[17−19] All ligands are neutral and donated as L, with their protonated forms donated as HL^+, in this paper.

Scheme 1. Synthesis of 2,2′-(Trifluoroazanediyl)bis(*N*,*N*′-dimethylacetamide)

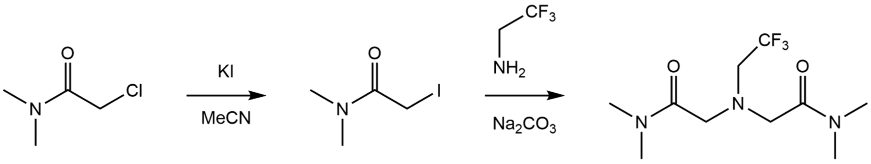

and physical properties. In addition, separation of uranium is always a significant task in the management of nuclear wastes and spent nuclear fuel reprocessing because uranium is the most abundant radioactive element in these processes. As a result, there has been substantial interest in the development of efficient ligands and extractants for the separation of actinides and lanthanides to help develop an advanced nuclear fuel cycle.

In the past two decades, a group of alkyl-substituted diglycolamides (DGA), including *N*,*N*,*N*′,*N*′-tetraoctyl-diglycolamide (TODGA),[5,6] *N*,*N*,*N*′,*N*′-tetraisobutyl-diglycolamide (TiBDGA),[7] and *N*,*N*′-dimethyl-*N*,*N*′-dihexyl-diglycolamide (DMDHDGA),[8] have become a subject of high interest in the area of actinide partitioning.[9] Actinides in nitric acid solutions can be effectively extracted into organic solvents containing these ligands and readily stripped back by diluted acid solutions.[5−12] In addition, the diglycolamide ligands are completely combustible because they are composed of only C, H, O, and N atoms. Therefore, the final amount of solid radioactive waste can be greatly reduced by using these CHON ligands to replace the traditional extractants containing phosphorus or sulfur. To help understand the thermodynamic and structural properties of the actinide complexes with DGA ligands, a number of studies have been conducted in recent years by using small alkyl groups (e.g., methyl) to render the DGA ligands water-soluble so that a variety of techniques, such as potentiometry, spectrophotometry, and calorimetry, are applicable to the studies.[13−16]

The alkyl-substituted DGA ligands are usually tridentate to the metal ions, using the two amide oxygen atoms and the center ether oxygen.[13−16] Considering that no substitutional groups can be attached to the ether oxygen of DGA to vary the basicity and binding strength of the ligands, we have previously synthesized and conducted the studies of a series of structurally related amine-bridged diacetamide ligands, including 2,2′-(benzylazanediyl)bis(*N*,*N*′-dimethylacetamide) (BnABDMA), 2,2′-azanediylbis(*N*,*N*′-dimethylacetamide) (ABDMA), and 2,2′-(methylazanediyl)bis(*N*,*N*′-dimethylacetamide) (MABDMA).[17−19] The structures of these ligands are similar to that of *N*,*N*,*N*′,*N*′-tetramethyl- diglycolamide (TMDGA) but differ in the linkage between the two amide groups: the two amide groups are bridged by an amine group in the former but an ether oxygen in the latter. As a result, different substitutional groups (e.g., a benzyl group in BnABDMA, a proton in ABDMA, and a methyl group in MABDMA) can be attached to the amine nitrogen so that the basicity of the amine nitrogen and the binding strength of the amine-bridged diacetamides can be fine-tuned. It has been demonstrated that these ligands form stronger complexes with Nd^{3+},[17] UO_2^{2+},[18] or NpO_2^{+}[19] than TMDGA.[13,14,16] In a tridentate mode similar to the DGA ligands, the amine-bridged diacetamides coordinate to the metal ions via the two amide oxygen atoms and the central nitrogen.

Among the three amine-bridged diacetamide ligands that were previously studied, the metal binding strength generally follows the order: MABDMA > ABDMA > BnABDMA,[17−19] which is attributed to the electron-donating ability of the methyl group in MABDMA and the electron-withdrawing ability of the benzyl group in BnABDMA. In this work, a new diacetamide ligand with a CF_3- group substituting on the central nitrogen, 2,2′-(trifluoroazanediyl)bis(*N*,*N*′-dimethylacetamide) (CF_3ABDMA, Figure 1), was synthesized. The CF_3- group is known to be strongly electron-withdrawing, and we hypothesized that the attachment of the CF_3- group could make the electronegativity on the amine nitrogen even lower than that in BnABDMA. To test this hypothesis and extend the structure−property relationship in metal complexation with the amine-bridged diacetamides, thermodynamic properties of the complexation of CF_3ABDMA with UO_2^{2+}, Nd^{3+}, and NpO_2^{+} were determined by potentiometry and spectrophotometry. Techniques including density functional theory (DFT) computation, ^{19}F NMR, electrospray ionization mass spectrometry (ESI-MS), and X-ray crystallography were used to provide the structural information on the complexes. The thermodynamic and structural data from this work were discussed in comparison with the data for the three previously studied amine-bridged diacetamide ligands.

2. EXPERIMENTAL SECTION

2.1. Chemicals. 2,2′-(Trifluoroazanediyl)bis(*N*,*N*′-dimethylacetamide), denoted as CF_3ABDMA in this paper, was prepared according to Scheme 1. 2-Chloro-*N*,*N*-dimethylacetamide (13.4 g, 110 mmol) was added to a suspension of potassium iodide (18.2 g, 110 mmol) in acetonitrile (200 mL), and the mixture was stirred vigorously for 3 h at room temperature under an atmosphere of dry nitrogen to produce 2-iodo-*N*,*N*-dimethylacetamide *in situ*. 2,2,2-Trifluoroethylamine (5.0 g, 50 mmol) and sodium carbonate (28 g, 200 mmol) were then added, and the mixture was stirred for 6 h at room temperature followed by heating to reflux for 16 h. The mixture was cooled to room temperature, filtered, then the solvent removed under reduced pressure to give a viscous brown oil. The oil was extracted with chloroform (50 mL × 4), washed with 50 mL of water, 20 mL of portions of 10% $Na_2S_2O_3$ to remove I_2 until the solution was colorless, and 50 mL of brine. The solution was dried over magnesium sulfate, passed through a plug of neutral alumina, and the solvent slowly evaporated at room temperature to give CF_3ABDMA as a very pale yellow solid (4.25 g, 32%). ^1H NMR ($CDCl_3$, 500 MHz): $\delta = 2.94$ (s, 6H), 2.99 (s, 6H), 3.44 (q, $^3J_{HF} = 10$ Hz), 3.75 (s, 4H); ^{13}C NMR ($CDCl_3$, 500 MHz): $\delta = 35.7$, 36.7, 56.0, 169.8, CH_2CF_3 carbon atoms not observed; ^{19}F NMR ($CDCl_3$, 400 MHz): $\delta = -70.6$ (t, $^3J_{FH} = 10$ Hz).

Milli-Q water was boiled and cooled (to avoid CO_2 contamination) before being used for the preparation of all solutions. All experiments were conducted at 25 °C and an ionic strength of 1.0 M $NaNO_3$. The stock solutions of U(VI) and Nd(III) were prepared, respectively, by dissolving $UO_2(NO_3)_2{\cdot}H_2O(s)$ in dilute nitric acid solution and $Nd_2O_3(s)$ (Aldrich, 99.9%) in concentrated nitric acid solution (~10 M) under low heating followed by dilution with water. The concentrations of UO_2^{2+} and Nd^{3+} in the stock solutions were determined by complexometry titrations using ethylenediaminetetraacetic acid (EDTA).[20] The stock solution of Np(V) was prepared by following a procedure slightly modified from that described elsewhere.[21] The concentration of Np(V) was determined by the optical absorbance at 980.2 nm ($\varepsilon = 395\ M^{-1}\ cm^{-1}$). The concentrations of free acid in the stock solutions of U(VI), Nd(III), and Np(V) were determined by Gran's titration.[22] The stock solution of CF_3ABDMA was prepared by dissolving appropriate amount of the ligand in 1.0 M $NaNO_3$. The concentration of the ligand was calculated from the weight and verified by potentiometry. All chemicals are reagent grade or higher.

It is also noted that for potentiometric and spectrophotometric titrations, the ionic strength of solutions were controlled to be 1.0 M $NaNO_3$ through adding an appropriate amount of $NaNO_3$.

2.2. Potentiometry. Potentiometric titrations were conducted to determine the equilibrium constants of the protonation and complexation of the ligand with U(VI). The titration system, controlled by a computer, consists of a water-jacketed cell, a pH meter (Metrohm Model 713) equipped with a combination pH electrode (Orion Model 8102), and an automatic buret (Metrohm Model 765). The titrations were conducted at a constant temperature (25.0 ± 0.1)°C. A constant flow of argon was applied over the solution to avoid contamination of CO_2. The pH electrode was filled with 1 M NaCl to reduce the electrode junction potential.

In acidic and basic regions, the electromotive force (E, in millivolts) can be expressed by eqs 1 and 2, respectively:

$$E = E^0 + RT/F\ \ln[H^+] + \gamma_H[H^+] \tag{1}$$

$$E = E^0 + RT/F\ \ln(Q_w/[OH^-]) + \gamma_{OH}[OH^-] \tag{2}$$

where the electrode parameters, E^0, γ_H, and γ_{OH}, were determined by an acid−base calibration titration with standard HCl and NaOH solutions prior to each titration. In eqs 1 and 2, T is the temperature in Kelvin, F is the Faraday constant, R is the gas constant, and $Q_w = [H^+][OH^-]$; the value of Q_w is $10^{-13.77}$ for the ionic medium of 1.0 M $NaNO_3$ in this work.

Duplicate or triplicate titrations were conducted with solutions of varying concentrations of the ligand, acidity, and U(VI). For the determination of the protonation constant of the ligand, the cup solution containing the ligand at different acidities was titrated with NaOH or HNO_3. For the determination of the equilibrium constants of the complexation with U(VI), the cup solution containing U(VI) and the ligand in an acidic solution was titrated with NaOH. The nonlinear regression program Hyperquad 2008 was used to fit the data and obtain the equilibrium constants.[23]

2.3. Spectrophotometry. Spectrophotometry was used to study the complexation of CF_3ABDMA with U(VI), Nd(III) and Np(V). Absorption spectra of U(VI) (350−550 nm, 0.2 nm interval), Nd(III) (560−610 nm, 0.2 nm interval), and Np(V) (950−1065 nm, 0.2 nm interval) were collected on a Cary 6000i UV−vis-NIR spectrophotometer (Varian Inc.) equipped with sample holders that were maintained at constant temperatures. Quartz cells with 10 mm optical path were used. Solutions containing the metal ions, U(VI), Nd(III) or Np(V), were placed in the cell and titrated with a solution of the ligand. A magnetic stir bar was previously placed into the cell. After each addition of ligand solution, the cell solution was thoroughly mixed by stirring for 1−2 min before the spectrum was collected. The mixing time is sufficient because prior studies have shown the absorbance became stable within 30 s of mixing. Usually, a set of 16−21 spectra were generated in one titration (with 15−20 additions of the titrant). The commercially available HypSpec program was used to analyze the data.[23]

2.4. ^{19}F NMR. To help evaluate the coordination of CF_3ABDMA with UO_2^{2+} and Nd^{3+}, ^{19}F NMR spectra of a few solution samples were acquired on a Bruker AVQ-400 instrument with a quad-channel probe. The samples include aqueous or methanol solutions of CF_3ABDMA in the absence or presence of metal ions UO_2^{2+} and La^{3+} (the latter is used as the analog of Nd^{3+} because it is diamagnetic). To verify the purity of the CF_3ABDMA, ^1H and ^{13}C NMR spectra were acquired on a Bruker DRX-500 instrument with a Z-gradient proton/BBO probe.

2.5. X-ray Crystallography. Pale yellow crystals of the 1:2 (U(VI):L) complex, $UO_2L_2(ClO_4)_2$, were obtained from 0.5 mL of aqueous solution containing 1 mM UO_2^{2+} and 5 mM ligand at pH ≈ 6. The solution was placed in a small glass vial, and the vial was loosely capped for slow evaporation. Crystallographic data were collected on Beamline 11.3.1 (for Small-Crystal Crystallography) at the Advanced Light Source of Lawrence Berkeley National Laboratory (LBNL), with the Bruker APEX II CCD diffractometer of ω rotation with narrow frames at a wavelength of 0.77490 Å. Intensity data were collected using Bruker Apex 2 software.[24] The Bruker SAINT software package was used to perform intensity data integration, cell refinement, and data reduction.[25] The crystal structure was solved using SHELXT and refined with SHELXL-2014.[26] Hydrogen atoms were placed using a riding model, with freely refined torsion angles where relevant. A high peak of residual density was found to remain proximate to the uranium center, but attempts to detect a second domain or merohedral twin were not successful. On the basis of the size of this peak (ca. 4 electrons) and the atomic number of uranium (95), any twin component is likely to account for only a small amount of the diffraction, explaining the difficulty in modeling it. Details of the crystallographic data are in Table 1.

2.6. ESI-MS. Electrospray ionization-mass spectrophotometry (ESI-MS) experiments were performed to identify U(VI)/CF_3ABDMA complexes on an Agilent 6340 quadrupole ion trap mass spectrophotometer equipped with a micro electrospray ionization (ESI) source. Ethanol−water (<5% water) was used as a spray solvent in the experiments. The spray solution of U(VI)/CF_3ABDMA complexes was prepared through diluting the U(VI)/CF_3ABDMA aqueous solution with the spray solvent by more than 100 times. The aqueous solution contained 2 mM U(VI) and 10 mM ligand with the pH around 3.0. The instrument has a detection range of 50−2200 m/z with a resolution of ~0.25 m/z in high resolution mode. The instrument parameters used to obtain the MS spectra of the complexes were similar to those previously employed.[17,18]

2.7. DFT Computational Studies. The three-parameter hybrid functional B3LYP[27,28] was used. Previous studies have demonstrated that reliable structural and energetic results were obtained for actinide complexes.[18,29,30] The metal ions and other elements were treated, respectively, with Stuttgart-Dresden small-core quasi-relativistic effective core potentials and a 6-31++G(d,p) Gaussian-type basis set. The polarizable continuum model (PCM) was used to take into account the solvent effect.[31] Geometry optimizations of the ligand as well as the complexes were performed with no symmetry constraints in PCM solvent. In the calculation of the free energies of metal complexes, the zero-point energy and thermal corrections including electronic, harmonic vibrational, rotational, and translational contributions to the internal energy were added to the electronic energy of each complex. In the calculation of the reaction free energies in solution, the correction was made for the standard state.[18,32] Gaussian 16 was used in all calculations.[33]

DOI: 10.1021/acs.inorgchem.9b02469
Inorg. Chem. XXXX, XXX, XXX−XXX

Table 1. Crystallographic Data and Structural Refinement

U(VI) complex	$UO_2L_2(ClO_4)_2$
empirical formula	$C_{20}H_{36}F_6Cl_2N_6O_{14}U$
formula weight	1007.48
temperature	100(2) K
wavelength	0.7749 Å
crystal system	monoclinic
space group	$P\ 2_1/c$
unit cell dimensions	a = 9.037(10), b = 14.372(16), c = 13.640(16), α = 90°, β = 107.783(12)°, γ = 90°
volume	1687(3) $Å^3$
Z	2
density (calculated)	1.984 Mg/m^3
absorption coefficient	2.906 mm^{-1}
F(000) color, habit	980 colorless, needle
crystal size (mm^3)	0.080 × 0.020 × 0.020
theta range for data collection	2.31 to 44.12°
index ranges	$-16 \le h \le 16 - 24 \le k \le 25 - 24 \le l \le 24$
reflections collected	35 321
independent reflections	7622 [R(int) = 0.0363]
completeness to theta = 27.706°	100%
absorption correction	eemiempirical from equivalents
max. and min transmission	0.7458 and 0.4235
refinement method	full-matrix least-squares on F^2
data/restraints/parameters	10100/0/227
goodness-of-fit on F^2	1.057
final R indices [I > 2sigma(I)]	$R1$ = 0.0328 $wR2$ = 0.0886
R indices (all data)	$R1$ = 0.0446 $wR2$ = 0.0967
extinction coefficient	n/a
largest diff. peak and hole	4.173 and −3.947 e $Å^{-3}$

3. RESULTS

3.1. Protonation of the Ligand. Experimental conditions and plots of the protonation titrations are shown in Table S1 and Figure S1 in the Supporting Information. The protonation constant of CF_3ABDMA (log K) is calculated to be 4.00 ± 0.09. This value is lower than those for the three previously studied amine-bridged ligands (Table 2). A trend in log K is observed as CF_3ABDMA < BnABDMA < ABDMA < MABDMA. Because the protonation of all these ligands occurs on the central amine N atom, the trend in log K reflects the order of basicity on N. Among the ligands, CF_3ABDMA has the lowest basicity due to the strong electron-withdrawing ability of the CF_3- groups.

Table 2. Protonation of CF_3ABDMA in Comparison to BnABDMA, ABDMA, and MABDMA ($H^+ + L = HL^+$) at 25 °C and I = 1.0 M $NaNO_3$[a]

ligand	log K	ref
CF_3ABDMA	4.00 ± 0.09	p.w.
BnABDMA	6.36 ± 0.09	17
ABDMA	7.12 ± 0.09	17
MABDMA	7.64 ± 0.09	17

[a] p.w. indicates present work.

3.2. Complexation of U(VI) with CF_3ABDMA. A representative potentiometric titration is shown in Figure 2.

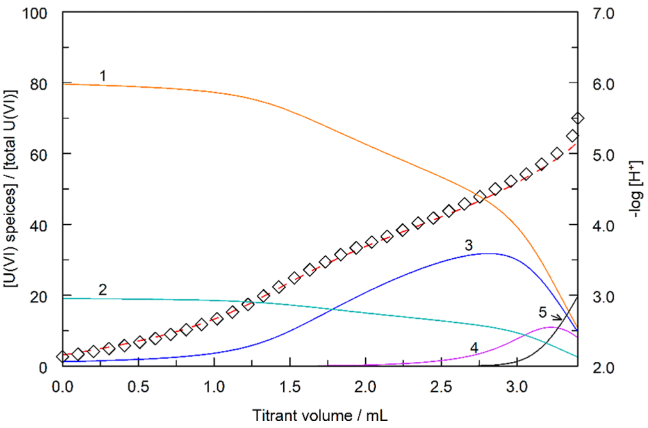

Figure 2. Potentiometric titration (Titration #3, the conditions are shown in Table S2, Supporting Information) of U(VI)/L complexation at 25 °C and I = 1.0 M $NaNO_3$. Symbols: (◊) experimental−log[H^+]; (dashed line) fitted−log[H^+]; (solid lines) U(VI) speciation, 1, free UO_2^{2+}; 2, $UO_2(NO_3)^+$; 3, UO_2L^{2+}; 4, $(UO_2)_2(OH)_2^{2+}$; 5, $(UO_2)_3(OH)_5^+$. The amount of $UO_2(OH)^+$ was too small to be shown in the figure.

The titration curve is best fitted with the model including the formation of 1:1 U(VI) complex, UO_2L^{2+} as shown in reaction 3. In the calculation, the protonation constant of CF_3ABDMA from this work, the stability constant of $UO_2(NO_3)^+$,[34] and the hydrolysis constants of three U(VI)/OH species, $UO_2(OH)^+$, $(UO_2)_2(OH)_2^{2+}$, and $(UO_2)_3(OH)_5^+$,[35] were also included. The calculated equilibrium constant for UO_2L^{2+} is shown in Table 3. The data are compared with those for Nd^{3+} and NpO_2^+ and with other related diacetamide ligands in subsequent sections:

$$UO_2^{2+} + L = [UO_2L]^{2+} \tag{3}$$

Table 3. Overall Equilibrium Constants for Complexation of CF_3ABDMA with UO_2^{2+}, Nd^{3+}, and NpO_2^+ at 25 °C and I = 1.0 M $NaNO_3$[a]

metal ion	reaction	method	log β
UO_2^{2+}	$UO_2^{2+} + L = UO_2L^{2+}$	pot	(2.05 ± 0.12)
Nd^{3+}	$Nd^{3+} + L = NdL^{3+}$	sp	(1.44 ± 0.09)
	$Nd^{3+} + 2L = NdL_2^{3+}$		(1.90 ± 0.09)
NpO_2^+	$NpO_2^+ + L = NpO_2L^+$	sp	(0.46 ± 0.09)

[a] Method: pot, potentiometry; sp, spectrophotometry.

Because a 1:2 U(VI)/CF_3ABDMA complex, $UO_2L_2(ClO_4)_2$, was obtained in the form of single crystal from aqueous solution (see sections 2.5 and 4.2), efforts were made to identify and determine the stability constant of 1:2 U(VI)/CF_3ABDMA complex in aqueous solution, $UO_2L_2^{2+}$ by potentiometry as well as spectrophotometry. The efforts were not successful due to the following reasons. With potentiometry, higher ratios of [L]/[U] were used to facilitate the formation of $UO_2L_2^{2+}$. Under such conditions, the protonation of the ligand dominates the titration and the change in [H^+] becomes insensitive to the formation of

U(VI)/CF_3ABDMA complexes. With spectrophotometry, a number of hydrolyzed U(VI) species that have significant optical absorption, including UO_2OH^+, $(UO_2)_2(OH)_2^{2+}$, and $(UO_2)_3(OH)_5^+$, must be included in fitting the overall spectra, which proved to be extremely difficult. As a result, in aqueous solution, only the stability constant of the 1:1 U(VI)/CF_3ABDMA complex was obtained in this work.

3.3. Complexation of Nd(III) with CF_3ABDMA. Figure 3 shows a representative set of absorption spectra for the titration of Nd(III) with CF_3ABDMA. With the addition of CF_3ABDMA, the intensities and positions of the branches of the absorption band varied as the ligand to metal ratio (L/Nd(III)) was increased. Factor analysis of the absorption spectra by the HypSpec program indicates that there are four absorbing species of Nd(III) including the free Nd^{3+} and $Nd(NO_3)^{2+}$ complex that were present in the beginning of the titration. Accordingly, the spectra were best-fitted with the formation of two successive Nd(III)/CF_3ABDMA complexes, as shown by reaction 4:

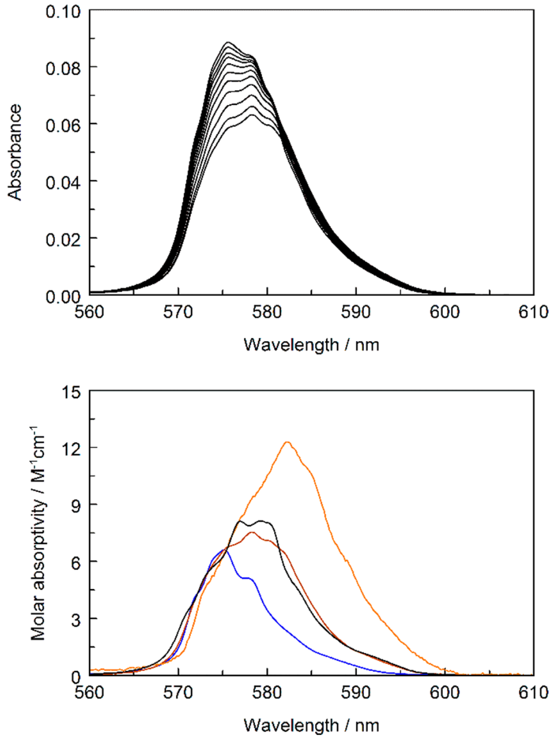

Figure 3. Spectrophotometric titrations of Nd^{3+} complexation with CF_3ABDMA (upper), and the calculated molar absorptivities of Nd(III) species (lower): Nd^{3+} (blue), $NdNO_3^{2+}$ (black), NdL^{3+} (brown), NdL_2^{3+} (rose). Detailed titration conditions are in Table S3 of the Supporting Information.

$$Nd^{3+} + nL = [NdL_n]^{3+} \tag{4}$$

where $n = 1$ and 2. The stability constants of the 1:1 and 1:2 complexes between Nd^{3+} and CF_3ABDMA were calculated to be 1.44 ± 0.09 and 1.90 ± 0.09, respectively. In the calculation, the pronation constant of CF_3ABDMA from this work and the stability constant of $Nd(NO_3)^{2+}$ from the literature[36] were used.

As shown in Table 3, the CF_3ABDMA complexes with both U(VI) and Nd(III) in aqueous solution are not strong and the U(VI) complex (log β_1 = 2.05) is stronger than that of Nd(III) (log β_1 = 1.44). These observations are corroborated by the ^{19}F NMR spectra shown in Figure S2 of the Supporting Information. The ^{19}F NMR data also show that the binding of CF_3ABDMA with UO_2^{2+} and La^{3+} becomes stronger in methanol solutions, which can be interpreted as the weaker solvation of metal ions in methanol than in water resulting in less energy required for desolvation. The ^{19}F NMR spectra and more detailed descriptions are provided in the Supporting Information.

3.4. Complexation of Np(V) with CF_3ABDMA. One representative set of absorption spectra in the spectrophotometric titration of Np(V) with CF_3ABDMA is shown in Figure 4. As the concentration of CF_3ABDMA increased, the intensity of the absorption band of free NpO_2^+ around 980.4 nm decreased, and a "shoulder" band appeared at about 988.0 nm. Analysis with the HypSpec program indicates that the spectral changes can be described by the formation of the 1:1 Np(V)/CF_3ABDMA as represented by reaction 5. Using the HypSpec program, the stability constant of the complex was calculated to be 0.46 ± 0.09. In the calculation, the pronation constant of CF_3ABDMA from this work and the stability constant of $NpO_2(NO_3)$ (aq) from the literature[37] were used:

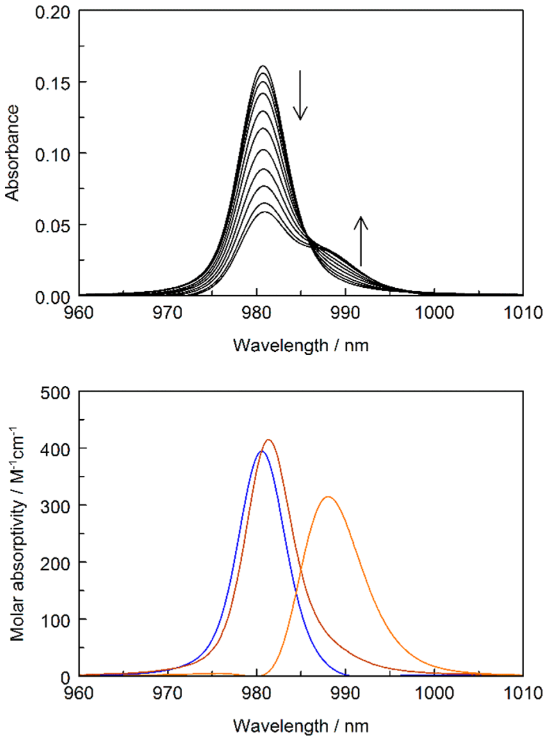

Figure 4. Spectrophotometric titrations of NpO_2^+ complexation with CF_3ABDMA (upper) and calculated molar absorptivity of Np(V) species (lower): NpO_2^+ (blue), NpO_2NO_3 (brown), NpO_2L^+ (rose). Detailed titration conditions are in Table S3 of the Supporting Information.

$$NpO_2^+ + L = NpO_2L^+ \tag{5}$$

4. DISCUSSION

4.1. Thermodynamic Trends. The stability constants of the complexes of CF_3ABDMA with UO_2^{2+}, Nd^{3+}, and NpO_2^+ from this work can be compared with the data of three structurally related diacetamide ligands, BnABDMA, ABDMA,

Table 4. Overall Equilibrium Constants for Complexation of CF_3ABDMA, in Comparison to BnABDMA, ABDMA, and MABDMA, with UO_2^{2+}, Nd^{3+}, and NpO_2^+ at 25 °C and I = 1.0 M $NaNO_3$

metal ion	ligand	reaction	log β	ref
UO_2^{2+}	CF_3ABDMA	$UO_2^{2+} + L = UO_2L^{2+}$	2.05 ± 0.12	p.w.
	BnABDMA	$UO_2^{2+} + L = UO_2L^{2+}$	4.33 ± 0.03	18
		$UO_2^{2+} + 2L = UO_2L_2^{2+}$	7.67 ± 0.06	
	ABDMA	$UO_2^{2+} + L = UO_2L^{2+}$	5.03 ± 0.03	18
		$UO_2^{2+} + 2L = UO_2L_2^{2+}$	9.08 ± 0.03	
	MABDMA	$UO_2^{2+} + L = UO_2L^{2+}$	5.30 ± 0.03	18
		$UO_2^{2+} + 2L = UO_2L_2^{2+}$	9.66 ± 0.03	
Nd^{3+}	CF_3ABDMA	$Nd^{3+} + L = NdL^{3+}$	1.44 ± 0.09	p.w.
		$Nd^{3+} + 2L = NdL_2^{3+}$	1.90 ± 0.09	
	BnABDMA	$Nd^{3+} + L = NdL^{3+}$	2.92 ± 0.09	17
		$Nd^{3+} + 2L = NdL_2^{3+}$	5.08 ± 0.09	
		$Nd^{3+} + 3L = NdL_3^{3+}$	7.13 ± 0.09	
	ABDMA	$Nd^{3+} + L = NdL^{3+}$	4.08 ± 0.09	17
		$Nd^{3+} + 2L = NdL_2^{3+}$	6.93 ± 0.09	
		$Nd^{3+} + 3L = NdL_3^{3+}$	10.02 ± 0.9	
	MABDMA	$Nd^{3+} + L = NdL^{3+}$	4.40 ± 0.09	17
		$Nd^{3+} + 2L = NdL_2^{3+}$	7.52 ± 0.36	
		$Nd^{3+} + 3L = NdL_3^{3+}$	10.50 ± 0.50	
NpO_2^+	CF_3ABDMA	$NpO_2^+ + L = NpO_2L^+$	0.46 ± 0.09	p.w.
	BnABDMA	$NpO_2^+ + L = NpO_2L^+$	2.90 ± 0.09	19
		$NpO_2^+ + 2L = NpO_2L_2^+$	4.01 ± 0.09	
	ABDMA	$NpO_2^+ + L = NpO_2L^+$	2.80 ± 0.09	19
		$NpO_2^+ + 2L = NpO_2L_2^+$	4.00 ± 0.09	
	MABDMA	$NpO_2^+ + L = NpO_2L^+$	3.59 ± 0.09	19
		$NpO_2^+ + 2L = NpO_2L_2^+$	5.50 ± 0.09	

and MABDMA, in the literature.[17−19] The data are summarized in Table 4. Two trends can be extracted from these data and discussed as follows.

4.1.1. Comparison between CF_3ABDMA, BnABDMA, ABDMA, and MABDMA. In Figure 5, the stability constants for the 1:1 complexes are plotted. For each metal ion, the binding strength of the four amine-bridged diacetamide ligands follows the trend MABDMA > ABDMA > BnABDMA > CF_3ABDMA, except for the complexation of Np(V) where ABDMA and BnABDMA show very similar binding strength. This trend is in accordance with the decrease in the basicity of the ligands as reflected by their protonation constants (Table 2). Both the trifluoromethyl and the phenyl groups have the electron-withdrawing ability, which reduces the electron density on the central N atom of CF_3ABDMA and BnABDMA ligands, in comparison with ABDMA. As a result, the basicity of CF_3ABDMA and BnABDMA is less than that of ABDMA, resulting in weaker complexes with CF_3ABDMA and BnABDMA than those with ABDMA. The complexation of CF_3ABDMA with the metal ions is the weakest among the four amine-bridged diacetamides, implying that the electron-withdrawing ability of the trifluoromethyl group is even stronger than that of the phenyl group. On the contrary, the methyl group has the electron-donating ability, which makes MABDMA a more basic ligand. Therefore, the metal complexes with MABDMA are stronger than those with ABDMA, and are the strongest among the complexes with all four diacetamides.

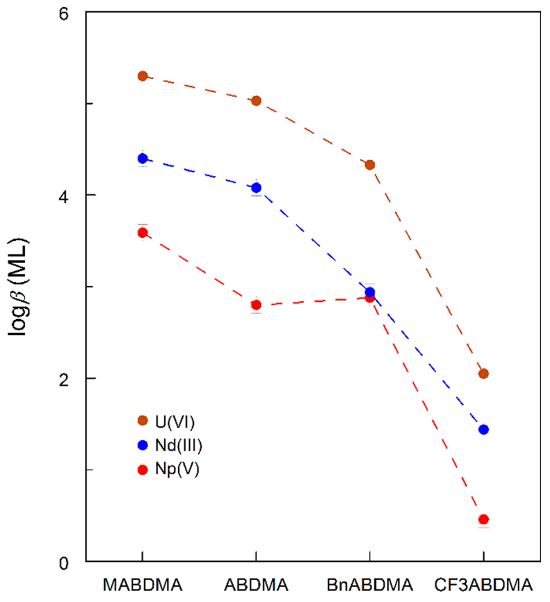

Figure 5. Thermodynamic trends in the complexation of amine-bridged diacetamide ligands with UO_2^{2+}, Nd^{3+}, and NpO_2^+. Data are for t = 25 °C and I = 1.0 M $NaNO_3$.

4.1.2. Comparison between UO_2^{2+}, Nd^{3+}, and NpO_2^+. Figure 5 also shows that, for each ligand, the stability constants of the 1:1 complexes follow the order: $UO_2^{2+} > Nd^{3+} > NpO_2^+$. This agrees with the order of the effective charges on the metal ions: + 3.2 (UO_2^{2+}) > + 3.0 (Nd^{3+}) > + 2.2 (NpO_2^+).[38] Such agreement may imply that the complexation of the amine-bridged diacetamides with actinide and lanthanide ions is predominantly electrostatic in nature.

It should be pointed out that when a ligand presents the same coordination mode to metal cations, a good correlation between the stability constants and effective charges is observed only if the complexation is dominantly electrostatic in nature. Other factors, including the degree of covalency and steric effects, must be taken into consideration when interpreting results for other complexation systems.

4.2. Coordination Modes. *4.2.1. Single Crystal Structure of $UO_2L_2(ClO_4)_2$.* In a previous study[18] of U(VI) complexation with MABDMA, ABDMA, and BnABDMA, EXAFS and computations suggested that amine-bridged diacetamides form tridentate complexes with U(VI) via the amine N atom and the two amide O atoms. No crystal structures of the U(VI)/diacetamide complexes were obtained in previous studies.

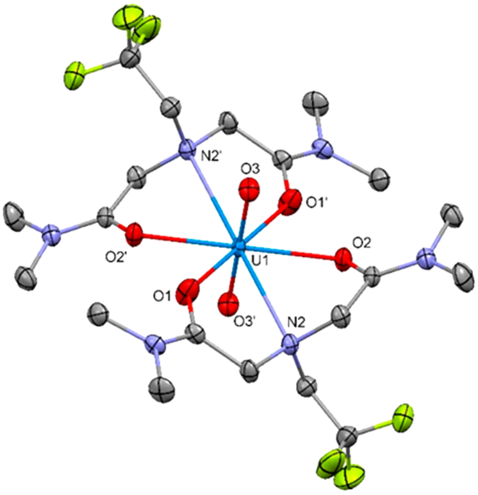

Figure 6. X-ray crystal structure of $UO_2L_2(ClO_4)_2$ with 50% probability ellipsoids. Perchlorate ions and hydrogen atoms are omitted for clarity.

The structure of $UO_2L_2(ClO_4)_2$ (Figure 6) obtained in this work is the first single crystal structure of a U(VI)/diacetamide complex. The structural data have been deposited as CCDC 1584249 in the Cambridge Crystallographic Data Centre (https://www.ccdc.cam.ac.uk/). The perchlorate salt of the dicationic 1:2 U(VI) complex with CF_3ABDMA was found to crystallize in the monoclinic space group $P2_1/c$, with the uranium atom lying directly on a crystallographic inversion center such that one-half of the complex generates the other by symmetry. Akin to the other uranyl complexes of this class of diacetamide ligands, CF_3ABDMA binds to the U(VI) center as a neutral species in a tridentate fashion.[14,18] A direct comparison of the bonding parameters of the U(VI)/CF_3ABDMA complex with those of the previously reported U(VI) complex of the diacetamide chelator TMDGA, which contains an ether (O) linkage in place of the functionalized amine nitrogen ($N-CH_2-CF_3$) found in CF_3ABDMA, can provide a basis for rationalizing the relative donor properties of these two ligands. The relevant crystallographically determined bond lengths for both complexes are given in Table 5. While a comparison of the $U-N_{amine}$ and $U-O_{ether}$ distances in these two complexes would be imprudent, the shorter $U-O_{amide}$ and longer $U-O_{uranyl}$ distances in the CF_3ABDMA complex indicate that despite the diminished basicity of its amine group, CF_3ABDMA is still a stronger ligand for U(VI) than TMDGA. This conclusion, as derived from the crystallographic data, aligns with the measured formation constants for the complexes as presented in this work and in previous work describing the TMDGA ligand.[14]

Table 5. Selected Bond Distances (Å) in $UO_2L_2(ClO_4)_2$ where L Stands for CF_3ABDMA in This Work or TMDGA[a]

bond	CF_3ABDMA	TMDGA[14]
U1−O1 (amide)	2.335(3)	2.416(4)
U1−O2 (amide)	2.386(3)	2.421(3)
U1−O3 (uranyl)	1.766(2)	1.752(3)
U1−N2 (amine) for CF_3ABDMA or U1−O (ether) for TMDGA	2.881(3)	2.614(3)

[a] Atom labels align to those given in Figure 4, with the corresponding functionalities specified in parentheses.

It needs some explanations for why the 1:2 U(VI)/CF_3ABDMA complex was obtained in crystal form but not identified in aqueous solution by potentiometry or spectrophotometry. We postulated that the formation of $UO_2L_2(ClO_4)_2$ is favored at higher pH (it in fact crystallized from a solution of pH ≈ 6, see section 2.5), but complications with the hydrolysis of U(VI) make it very difficult to observe and determine the formation constant of $UO_2L_2(ClO_4)_2$ in aqueous solution of high pH.

It is known that the hydrolysis of metal ions in a mixture of water/ethanol could be substantially suppressed, due to the much lower dissociation constants ($[H^+][OH^-]$) of such media than that of pure water.[39] Therefore, we hypothesized that the 1:2 U(VI)/CF_3ABDMA complex in solution could probably be observed in a mixture of water/ethanol. To test the validity of this hypothesis, ESI-MS experiments were conducted by spraying the U(VI)/ CF_3ABDMA solution (<5% water in ethanol) into the instrument. Indeed, the 1:2 U(VI) complex with CF_3ABDMA was observed as a doubly charged species, $UO_2L_2^{2+}$, by ESI-MS experiments. Detailed results from ESI-MS were provided in Supporting Information (Figure S2).

4.2.2. DFT Calculations. It has been previously[18] shown that for the UO_2^{2+}/diacetamide complexes, two types of minima of similar energy exist, differing in the conformation of the diacetamide ligand: Type *a* with a "distorted" O−C··C−O dihedral angle ~ 30° and Type *b* with a "planar" O−C··C−O dihedral angle ~ 0° (see Figure 5 of ref 18). In this work, for simplicity, only the complexes with "distorted" ligands were computed.

DFT calculations were performed for the 1:1 and 1:2 UO_2^{2+}/CF_3ABDMA complexes by following the same stepwise approach that was detailed in a previous study including optimization of structures, calculation of minimum energy of the complexes in gas phase and water, and calculation of the free energy for theoretical complexation reactions 6 and 7 in water. The calculations also provide the ESP charges on the donor atoms of CF_3ABDMA in the free and complexed ligand that help to explain the binding strength of CF_3ABDMA in comparison with other diacetamide ligands previously studied:

$$[UO_2(H_2O)_5]^{2+} + L \rightarrow [UO_2L(H_2O)_3]^{2+} + 2H_2O \quad (6)$$

$$[UO_2L(H_2O)_3]^{2+} + L \rightarrow [UO_2L_2]^{2+} + 3H_2O \quad (7)$$

The theoretically calculated free energy for reactions 6 and 7 are shown in Table 6. Other computational results, including structure optimization, minimum energy of the complexes in gas phase and water, and the ESP charges on the donor atoms, are provided in the Supporting Information as Figure S3, Table S4, and Table S5.

Table 6. Theoretically Calculated Free Energies (ΔG_{water}) for Complex Formation (kcal mol^{-1}) for Reactions 6 and 7 in Comparison with Experimental Equilibrium Constants of Formation of U(VI)/Diacetamide Complexes[a]

reaction	ligand	ΔG_{water}	log K_{exp}	Δlog K_{calc}	Δlog K_{exp}	ref
6	CF_3ABDMA	−14.3	2.05	−3.7	−2.3	this work
	BnABDMA	−19.3	4.33	0	0	18
	ABDMA	−19.0	5.03	−0.2	0.7	18
	MABDMA	−21.0	5.30	1.2	1	18
7	CF_3ABDMA	−17.4	(1.8)[b]	−1.5	(−1.5)[b]	this work
	BnABDMA	−19.5	3.34	0	0	18
	ABDMA	−20.1	4.05	0.4	1.4	18
	MABDMA	−20.0	4.37	0.4	2	18

[a] Δlog K_{calc} = log K_{calc} (ligand) − log K_{calc} (BnABDMA), Δlog K_{exp} = log K_{exp} (ligand) − log K_{exp} (BnABDMA). [b] Estimated value from the calculated ΔG_{water} in this work.

As shown in Table 6, the calculated free energy for the formation of 1:1 U(VI)/CF_3ABDMA complex (−14.3 kcal mol^{-1}) is much less negative than those of the other diacetamide complexes (from −19.0 to −21.0 kcal mol^{-1}), in good agreement with the order of the experimentally determined equilibrium constants. The values of Δlog K in Table 6 are relative values for each ligand with respect to those of log K for BnABDMA. The correlation between the experimental and calculated Δlog *K* for the 1:1 U(VI)/diacetamide complexes is fairly good as shown in Figure S4 in the Supporting Information.

The ESP charges for free CF_3ABDMA ligand and the U(VI) complexes are shown in Table S5. These data could be compared with those for the other three diacetamide ligands previously calculated at the same level of theory.[18] It should be noted that, in general, the relative stability of the complexes cannot be exclusively predicted by the charge on the central amine nitrogen. The solvation and steric effects induced by the substituents on the nitrogen atom are also the factors affecting the stability of the complex, as observed and discussed in the previous study.[18]

In brief, DFT calculations confirm that CF_3ABDMA is the weakest ligand among the four studied diacetamides. The calculated free energy for the formation of 1:2 U(VI)/CF_3ABDMA complex (−17.4 kcal mol^{-1}) is also less than those of the other diacetamide complexes (from −19.5 to −20.1 kcal mol^{-1}). In the absence of experimentally determined equilibrium constant for the formation of 1:2 U(VI)/CF_3ABDMA complex, we could, using the trends of values for reaction 7 in Table 6, estimate that the log K_{exp} for the stepwise formation of 1:2 U(VI)/CF_3ABDMA complex is about 1.8.

5. CONCLUSION

A new member of the series of amine-bridged diacetamide ligands, 2,2′-(trifluoroazanediyl)bis(*N*,*N*′-dimethylacetamide) (CF_3ABDMA), was synthesized, and its complexation with three metal ions, UO_2^{2+}, Nd^{3+}, and NpO_2^+, was studied with thermodynamic, structural, and computational techniques. With each of the three metal ions, CF_3ABDMA was found to form the weakest complexes among the four amide-bridged diacetamides, presumably due to the strong electron withdrawing character of the CF_3- group that reduces the basicity of the amine nitrogen. The binding strength of the four diacetamide ligands with UO_2^{2+}, Nd^{3+}, and NpO_2^+ follows the order of the effective electronic charge on the metal ions, indicating the complexation of amine-bridged diacetamides with these cations is predominantly electrostatic interactions.

■ ASSOCIATED CONTENT

Supporting Information

The Supporting Information is available free of charge on the ACS Publications website at DOI: 10.1021/acs.inorgchem.9b02469.

Experimental conditions of potentiometric and spectrophotometric titrations, ^{19}F NMR data, ESI-MS data, and DFT computation (PDF)

■ AUTHOR INFORMATION

Corresponding Authors

*E-mail: lxzhang@lbl.gov. Phone: 1-510-486-5142. Fax: 1-510-486-5596.
*E-mail: lrao@lbl.gov.

ORCID

Trevor D. Lohrey: 0000-0003-3568-7861
John K. Gibson: 0000-0003-2107-5418
John Arnold: 0000-0001-9671-227X
Zhicheng Zhang: 0000-0002-2192-3846
Linfeng Rao: 0000-0002-1873-0066

Notes

The authors declare no competing financial interest.

■ ACKNOWLEDGMENTS

The thermodynamic measurements, ESI-MS experiments, and X-ray crystallographic work are supported by the U.S. Department of Energy (DOE), Office of Science, Office of Basic Energy Sciences, under Contract No. DE-AC02-05CH11231 at LBNL. Single-crystal X-ray diffraction data were collected and analysed at the Advanced Light Source (ALS) that is supported by the Director, Office of Science, Office of Basic Energy Sciences, U.S. DOE under Contract No. DE-AC02-05CH11231. The collection of NMR data is supported by the UC Berkeley NMR facility, funded in part by NSF grants CHE 9633007, CHE 82-08992, and NIH grants 1S10RR016634-01 and RR 02424A-01. Y.G. acknowledges financial support from the China Scholarship Council for her visit to LBNL. T.D.L. thanks the U.S. DOE Integrated University Program for a graduate research fellowship. A.M. acknowledge the support for the computational studies by the "Piano Strategico d'Ateneo 2016-18" Program at University of Udine, Italy.

■ REFERENCES

(1) Nash, K. L.; Choppin, G. R. Separations Chemistry for Actinide Elements: Recent Developments and Historical Perspective. *Sep. Sci. Technol.* **1997**, *32* (1−4), 255−274.

(2) Sood, D. D.; Patil, S. K. Chemistry of Nuclear Fuel Reprocessing: Current Status. *J. Radioanal. Nucl. Chem.* **1996**, *203* (2), 547−573.

(3) *Yucca Mountain Science and Engineering Report Rev. 1*; U. S. Department of Energy: North Las Vegas, 2002.

(4) Yoshida, Z.; Johnson, S. G.; Kimura, T.; Krsul, J. R. In *The Chemistry of the Actinide and Transactinide Elements*; 3rd ed.; Morss, L. R., Edelstein, N. M., Fuger, J., Eds.; Springer: Dordrecht, The Netherlands, 2008; Chapter 6, Vol. *2*, pp 699−812.

(5) Suzuki, H.; Sasaki, Y.; Sugo, Y.; Apichaibukol, A.; Kimura, T. Extraction and Separation of Am(III) and Sr(II) by N,N,Ń,Ń-Tetraoctyl-3-Oxapentanediamide (TODGA). *Radiochim. Acta* **2004**, *92* (8), 463−466.

(6) Ansari, S. A.; Pathak, P. N.; Husain, M.; Prasad, A. K.; Parmar, V. S.; Manchanda, V. K. Extraction of Actinides Using N,N,N′,N′-Tetraoctyl Diglycolamide (TODGA): A Thermodynamic Study. *Radiochim. Acta* **2006**, *94* (6−7), 307−312.

(7) Tian, G.; Zhang, P.; Wang, J. C.; Rao, L. Extraction of Actinide(III, IV, V, VI) Ions and TcO4- by N,N,N',N'-Tetraisobutyl-3-Oxa-Glutaramide. *Solvent Extr. Ion Exch.* **2005**, *23* (5), 631−643.

(8) Sasaki, Y.; Choppin, G. R. Extraction of Np(V) by N,N'-Dimethyl-N,N'-Dihexyl-3-Oxapentanediamide. *Radiochim. Acta* **1998**, *80* (2), 85−88.

(9) Ansari, S. A.; Pathak, P. N.; Mohapatra, P. K.; Manchanda, V. K. Chemistry of Diglycolamides: Promising Extractants for Actinide Partitioning. *Chem. Rev.* **2012**, *112* (3), 1751−1772.

(10) Nave, S.; Modolo, G.; Madic, C.; Testard, F. Aggregation Properties of N, N, N′, N′-Tetraoctyl-3-oxapentanediamide (TODGA) in n-Dodecane. *Solvent Extr. Ion Exch.* **2004**, *22* (4), 527−551.

(11) Narita, H.; Yaita, T.; Tachimori, S. Extraction of Lanthanides with N, N′-Dimethyl-N, N′-diphenyl-malonamide and −3,6-dioxaoctanediamide. *Solvent Extr. Ion Exch.* **2004**, *22* (2), 147−161.

(12) Shimada, A.; Yaita, T.; Narita, H.; Tachimori, S.; Okuno, K. Extraction Studies of Lanthanide(III) Ions with N, N′-Dimethyl-N, N′-diphenylpyridine-2,6-dicarboxyamide (DMDPhPDA) from Nitric Acid Solutions. *Solvent Extr. Ion Exch.* **2004**, *22* (2), 147−161.

(13) Tian, G.; Xu, J.; Rao, L. Optical Absorption and Structure of a Highly Symmetrical Neptunium(v) Diamide Complex. *Angew. Chem., Int. Ed.* **2005**, *44* (38), 6200−6203.

(14) Tian, G.; Rao, L.; Teat, S. J.; Liu, G. Quest for Environmentally Benign Ligands for Actinide Separations: Thermodynamic, Spectroscopic, and Structural Characterization of UVI complexes with Oxa-Diamide and Related Ligands. *Chem. - Eur. J.* **2009**, *15* (16), 4172−4181.

(15) Rao, L.; Tian, G.; Teat, S. J. Complexation of Np(V) with N,N-Dimethyl-3-Oxa-Glutaramic Acid and Related Ligands: Thermodynamics, Optical Properties and Structural Aspects. *Dalton Trans.* **2010**, *39* (13), 3326−3330.

(16) Tian, G.; Teat, S. J.; Rao, L. Structural and Thermodynamic Study of the Complexes of Nd(III) with N,N,N′,N′-Tetramethyl-3-Oxa-Glutaramide and the Acid Analogues. *Inorg. Chem.* **2014**, *53* (18), 9477−9485.

(17) Dau, P. V.; Zhang, Z.; Dau, P. D.; Gibson, J. K.; Rao, L. Thermodynamic Study of the Complexation between Nd3+ and Functionalized Diacetamide Ligands in Solution. *Dalton. Trans.* **2016**, *45* (30), 11968−11975.

(18) Dau, P. V.; Zhang, Z.; Gao, Y.; Parker, B. F.; Dau, P. D.; Gibson, J. K.; Arnold, J.; Tolazzi, M.; Melchior, A.; Rao, L. Thermodynamic, Structural, and Computational Investigation on the Complexation between UO22+ and Amine-Functionalized Diacetamide Ligands in Aqueous Solution. *Inorg. Chem.* **2018**, *57* (4), 2122−2131.

(19) Gao, Y.; Dau, P. V.; Parker, B. F.; Arnold, J.; Melchior, A.; Zhang, P.; Rao, L. Complexation of NpO2+ with Amine-Functionalized Diacetamide Ligands in Aqueous Solution: Thermodynamic, Structural, and Computational Studies. *Inorg. Chem.* **2018**, *57*, 6965−6972.

(20) Dean, J. A. *Analytical Chemistry Handbook*; McGraw-Hill, Inc.: New York, 1995; pp 3−108.

(21) Rao, L.; Srinivasan, T. G.; Garnov, A. Y.; Zanonato, P.; Bernardo, P. D.; Bismondo, A. Hydrolysis of neptunium(V) at variable temperatures (10−85°C). *Geochim. Cosmochim. Acta* **2004**, *68* (23), 4821.

(22) Gran, G. Determination of the equivalence point in potentiometric titrations. Part II. *Analyst* **1952**, *77* (920), 661−671.

(23) Gans, P.; Sabatini, A.; Vacca, A. Investigation of equilibrium in solution. Determination of equilibrium constants with the Hyperquad suite of programs. *Talanta* **1996**, *43*, 1739−1753.

(24) *Apex2*; Bruker Analytical X-ray Systems Inc.: Madison, WI, 2003.

(25) *SAINT: SAX Area-Detector Integration Program v7.60a*; Bruker Analytical X-ray Systems, Inc.: Madison, WI, 2010.

(26) Sheldrick, G. M. A Short History of SHELX. *Acta Crystallogr., Sect. A: Found. Crystallogr.* **2008**, *64* (1), 112−122.

(27) Becke, A. D. A New Mixing of Hartree-Fock and Local Density-Functional Theories. *J. Chem. Phys.* **1993**, *98* (2), 1372−1377.

(28) Lee, C. T.; Yang, W. T.; Parr, R. G. Development of the Colle-Salvetti Correlation-Energy Formula Into A Functional of the Electron-Density. *Phys. Rev. B: Condens. Matter Mater. Phys.* **1988**, *37* (2), 785−789.

(29) Di Bernardo, P.; Zanonato, P. L.; Benetollo, F.; Melchior, A.; Tolazzi, M.; Rao, L. Energetics and Structure of Uranium(VI)-Acetate Complexes in Dimethyl Sulfoxide. *Inorg. Chem.* **2012**, *51* (16), 9045−9055.

(30) Endrizzi, F.; Melchior, A.; Tolazzi, M.; Rao, L. Complexation of Uranium(VI) with Glutarimidoxioxime: Thermodynamic and Computational Studies. *Dalt. Trans.* **2015**, *44* (31), 13835−13844.

(31) Tomasi, J.; Mennucci, B.; Cammi, R. Quantum Mechanical Continuum Solvation Models. *Chem. Rev.* **2005**, *105* (8), 2999−3093.

(32) Vukovic, S.; Hay, B. P.; Bryantsev, V. S. Predicting Stability Constants for Uranyl Complexes Using Density Functional Theory. *Inorg. Chem.* **2015**, *54* (8), 3995−4001.

(33) Frisch, M. J. G.; Trucks, W.; Schlegel, H. B.; Scuseria, G. E.; Robb, M. A.; Cheeseman, J. R.; Scalmani, G.; Barone, V.; Mennucci, B.; Petersson, G. A.; Nakatsuji, H.; Caricato, M.; Li, X.; Hratchian, H. P.; Izmaylov, A. F.; Bloino, J.; Zheng, G.; Sonnenberg, J. L.; et al. *Gaussian 16*, Rev. A.03, Gaussian, Inc.: Wallingford, CT, 2016.

(34) Rao, L.; Tian, G. Thermodynamic Study of the Complexation of Uranium(VI) with Nitrate at Variable Temperatures. *J. Chem. Thermodyn.* **2008**, *40* (6), 1001−1006.

(35) Zanonato, P.; Bernardo, P. D.; Bismondo, A.; Liu, G.; Chen, X.; Rao, L. Hydrolysis of Uranium(VI) at Variable Temperatures (10−85 °C). *J. Am. Chem. Soc.* **2004**, *126*, 5515−5522.

(36) Rao, L.; Tian, G. Complexation of Lanthanides with Nitrate at Variable Temperatures: Thermodynamics and Coordination Modes. *Inorg. Chem.* **2009**, *48* (3), 964−970.

(37) Vasudeva Rao, P.R.; Gudi, N.M.; Bagawde, S.V.; Patil, S.K. The complexing of Np(V) by some inorganic ligands. *J. Inorg. Nucl. Chem.* **1979**, *41* (2), 235−239.

(38) Choppin, G. R.; Rao, L. F. Complexation of Pentavalent and Hexavalent Actinides by Fluoride. *Radiochim. Acta* **1984**, *37* (3), 143−146.

(39) Rondinini, S.; Longhi, P.; Mussini, P. R.; Mussini, T. Autoprotolysis constants in non-aqueous solvents and aqueous organic solvent mixtures. *Pure Appl. Chem.* **1987**, *59* (12), 1693−1702.

DOI: 10.1021/acs.inorgchem.9b02469